

# Imidazole Catalyses in Aqueous Systems. VI. The Enzyme-Like Catalysis in the Hydrolysis of a Phenyl Ester by Phenylimidazole-Containing Copolymers. The Correlation between Binding Capacity and Catalytic Activity

Toyoki Kunitake\* and Seiji Shinkai

Contribution No. 215 from the Department of Organic Synthesis, Faculty of Engineering, Kyushu University, Fukuoka 812, Japan.

Received July 9, 1970

**Abstract:** Hydrolyses of *p*-acetoxybenzoic acid catalyzed by copolymers of *N*-[*p*-4(5)-imidazolylbenzyl]acrylamide (PI) were studied at 15–40° and mostly at pH 8.0 in 1.0 *M* aqueous KCl. The rate of the catalytic hydrolysis could be described by Michaelis–Menten kinetics showing leveling off of the rate at high substrate concentrations. On the other hand, the catalytic hydrolysis with a model compound of the catalytic unit, *p*-acetamidomethylphenyl-4(5)-imidazole, followed second-order kinetics. The PI–vinylpyrrolidone (PI–VP) copolymers showed smaller dissociation constants of the catalyst–substrate complex and smaller intracomplex rates than the PI–acrylamide (PI–AA) copolymers, reflecting an increased hydrophobic property of the catalytic site in PI–VP copolymers. The substrate binding with the polymer catalyst showed large negative entropy changes, supporting the supposition that the substrate binding is based on hydrophobic forces. The entropies of activation of the intracomplex process were unusually large negative values (–58 to –60 eu). When the reactivity difference of the imidazole group due to different *pK<sub>a</sub>* values was corrected according to Bruice and Schmir, the decrease in the free energy due to substrate binding was mostly offset by the increase in the free energy of activation of the intracomplex process. The interpretation of this result is that the hydrophobic interaction in the catalyst–substrate complex becomes destroyed in the transition state of the intracomplex reaction.

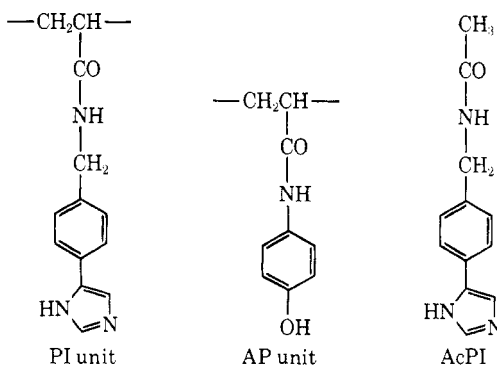
In the previous publications of the present series,<sup>1–5</sup> we showed that several imidazole-containing compounds, small molecules as well as macromolecules, catalyzed the hydrolysis of phenyl esters by way of the Michaelis–Menten kinetics. Interestingly, the structure and activity of the catalytic site were dependent upon the combination of various monomer units. Therefore, it is interesting to know the relationship, if any, between the binding capability and the catalytic efficiency of these catalytic systems, as in enzymatic reactions. In this paper, we extended the investigation to polymer catalysts containing a phenylimidazole (PI) unit and a phenol (AP) unit, and determined thermodynamic and activation parameters of the enzyme-like catalysis. At the same time, it was attempted to estab-

lish the above-mentioned correlation among the catalytic systems that we have studied so far.

## Experimental Section

**4(5)-[*p*-Cyanophenyl]imidazole.** The procedure for preparation of a naphthylimidazole<sup>6</sup> was essentially followed. In a 2-l. three-necked flask equipped with a mechanical stirrer and a reflux condenser, 112 g (1.0 mol) of selenium dioxide was dissolved in 1 l. of warm dioxane containing 40 ml of water. Then 145 g (1.0 mol) of *p*-cyanoacetophenone, mp 56–58° (lit.<sup>6</sup> 54–56°), was added quickly and the reaction mixture was stirred for 36 hr under reflux and for 16.5 hr at room temperature. The precipitated selenium metal was filtered and the solvent removed *in vacuo*. The residue, while warm, was dissolved in 600 ml of acetone and the precipitate formed (selenium metal) was filtered. Acetone was evaporated, the resulting yellow residue (*p*-cyanophenylglyoxal) dissolved in methanol, and methanol evaporated. Evaporation and addition of methanol were repeated two more times, in order to remove acetone completely. The methanol solution was used in several portions for the next step without further purification.

In a 1-l. three-necked flask equipped with a mechanical stirrer and a reflux condenser was dissolved 60 g (0.3 mol) of cupric acetate in 600 ml of 38% aqueous ammonia and 50 ml of 37% aqueous formaldehyde by stirring. *p*-Cyanophenylglyoxal (18 g, 0.11 mol, the quantitative conversion from *p*-cyanoacetophenone assumed) in 50 ml of methanol was added with stirring. Stirring was continued for 1 hr, and the copper salt of the imidazole compound was obtained as dark brown precipitates. The crude copper complex was treated with acetone for a few hours in a Soxhlet extractor, in order to remove tarry materials. The yield of the purified copper complex was 60–65%. With stirring, hydrogen sulfide was passed for 3 hr through a suspension of the copper complex in *ca.* 30 vol % of hot aqueous ethanol. Cupric sulfide was removed by filtration and washed with the aqueous ethanol. The solvent was removed from the combined solution and washings. The residual orange solid was taken up in 12 *N* hydrochloric acid, filtered, and treated three times with active charcoal, and the solvent removed *in vacuo*. There was thus obtained 4(5)-[*p*-cyanophenyl]imidazole hydrochloride, yield, *ca.* 60% based on the copper salt. Recrystallizations (twice with charcoal treatments) from 90% aqueous acetic acid gave pale yellow needles: mp 200–225°;



(1) (a) C. Aso, T. Kunitake, and F. Shimada, *J. Polym. Sci., Part B*, **6**, 467 (1968); (b) T. Kunitake, F. Shimada, and C. Aso, *J. Amer. Chem. Soc.*, **91**, 2716 (1969).

(2) T. Kunitake, F. Shimada, and C. Aso, *Makromol. Chem.*, **126**, 276 (1969).

(3) C. Aso, T. Kunitake, and S. Shinkai, *Chem. Commun.*, 1483 (1968); T. Kunitake, S. Shinkai, and C. Aso, *Bull. Chem. Soc. Jap.*, **43**, 1109 (1970).

(4) T. Kunitake and S. Shinkai, *ibid.*, **43**, 2581 (1970).

(5) T. Kunitake and S. Shinkai, *J. Amer. Chem. Soc.*, **93**, 4247 (1971).

(6) L. Friedman and H. Shechter, *J. Org. Chem.*, **26**, 2522 (1961).

**Table I.** Preparation of Polymer Catalysts<sup>a</sup>

Copolymer	Monomer, <i>M</i>			Polymerization time, min	Conversion, %	Polymer unit, mol %	
	PI	AA	AP			PI	AP
PI-AA-1	0.05	3.00		80	24.4	1.68	
PI-AA-2	0.10	1.00		80	20.1	8.91	
PI-AP-AA-1	0.05	2.00	0.05	100	32.0	2.0	Ca. 1.8
PI-AP-AA-2	0.05	2.00	0.15	100	28.6	1.7	5.0
PI-VP	0.03	3.00 <sup>b</sup>		40	26.0	1.94	

<sup>a</sup> 70°C; methanol solvent; AIBN initiator, 1/800 mol of the AA or VP comonomer. <sup>b</sup> VP comonomer.

ir (KBr) 3200–2800 (imidazole N–H), 2220 (cyano group), 1640, 1175 cm<sup>−1</sup> (imidazole ring). *Anal.* Calcd for C<sub>10</sub>H<sub>7</sub>N<sub>3</sub>·HCl: C, 58.38; H, 3.92; N, 20.45. Found: C, 58.23; H, 3.93; N, 19.77.

*N*-[*p*-(4(5)-imidazolyl)benzyl]acrylamide (PI Monomer). In a 200-ml three-necked flask equipped with a mechanical stirrer, a dropping funnel, and a reflux condenser connected to a calcium chloride tube were placed 4.5 g (0.15 mol) of lithium aluminum hydride and 150 ml of tetrahydrofuran (distilled from LiAlH<sub>4</sub>). A suspension of 5.1 g (0.03 mol) of finely powdered 4(5)-[*p*-cyano-phenyl]imidazole hydrochloride in 50 ml of tetrahydrofuran was added from a dropping funnel over 15 min with gentle refluxing. The reaction mixture turned green immediately. After stirring for an additional 2 hr under reflux, 50 ml of water was added from a dropping funnel and the mixture was then poured into 100 ml of 10% aqueous sodium hydroxide. A small amount of Rochelle salt was added to effect better phase separation. The pale yellow organic layer was separated, added with some hydrochloric acid, and the solvent evaporated *in vacuo*, leaving pale yellow needles as residues, yield 4.1 g (78%). The peak due to the cyano group did not appear in the ir spectrum, indicating its conversion to the aminomethyl group.

Since the solid amine product was unstable, the organic layer (tetrahydrofuran solution) was employed as such for the next step. The tetrahydrofuran solution in a 100-ml flask was cooled in an ice bath and added dropwise with 3 g (0.036 mol) of acrylyl chloride and 8 ml of 4 *N* aqueous sodium hydroxide simultaneously. The reaction mixture was stirred during the addition (20 min) and for the subsequent 40 min. Then the reaction mixture was adjusted to pH 4–5, concentrated to ca. 15 ml, and kept in a freezer (ca. −20°C). Fine flakes obtained in 45% yield were recrystallized from 3:1 (v/v) water-ethanol: mp 187–190°C; ir (KBr) 1660 (carbonyl), 1615 cm<sup>−1</sup> (vinyl). *Anal.* Calcd for C<sub>13</sub>H<sub>13</sub>N<sub>3</sub>O·H<sub>2</sub>O: C, 63.92; H, 6.19; N, 17.20. Found: C, 63.47; H, 5.97; N, 16.41.

4(5)-[*p*-Acetamidomethylphenyl]imidazole (AcPI). 4(5)-[*p*-Cyano-phenyl]imidazole (17 g, 0.01 mol) was reduced with lithium aluminum hydride in the same way as above. The resulting tetrahydrofuran solution of the aminomethyl product was added with 1.1 g (0.011 mol) of acetic anhydride and refluxed for 3 hr. A small amount of concentrated hydrochloric acid was added and the mixture was concentrated. The residual viscous oil was added to a saturated aqueous solution of sodium carbonate and pale yellow solids were recovered by centrifuge. Recrystallizations from water gave pale yellow needles in 42% yield, mp 146–148°C. *Anal.* Calcd for C<sub>12</sub>H<sub>13</sub>N<sub>3</sub>O·H<sub>2</sub>O: C, 61.78; H, 6.48; N, 18.01. Found: C, 61.20; H, 6.44; N, 17.67. The purity determined by titration of the imidazole group was 99.2%.

**Other Materials.** Preparation of the substrate, *p*-acetoxybenzoic acid, has been described previously.<sup>3</sup> Potassium chloride was dried before use. Urea was recrystallized from ethanol. De-ionized water was boiled before use to expel dissolved carbon dioxide.

**Titration and hydrolysis procedures** were already given.<sup>1b,3</sup>

**Preparations of Polymer Catalysts.** Copolymerizations were conducted in methanol at 70°C with azobisisobutyronitrile in sealed ampoules under nitrogen. The results are summarized in Table I. Polymerization was terminated after a given polymerization period by pouring the reaction mixture into excess ether. The acrylamide (AA) copolymers were reprecipitated from water and methanol (or from methanol and acetone) and the vinylpyrrolidone (VP) copolymers were reprecipitated from ethanol and ether. The copolymer compositions were determined by titration and infrared spectroscopy as described previously.<sup>5</sup>

**Viscosity Measurement.** The viscosity of polymer catalysts was measured at 30°C using a modified Ubbelohde viscometer. The viscosity data are summarized in Table II.

**Table II.** Intrinsic Viscosity of Polymer Catalysts

Copolymer	[ $\eta$ ], dl/g	
	1 <i>M</i> KCl	8 <i>M</i> urea
PI-AA-2	0.105	0.265
PI-AP-AA-2	0.212	0.455
PI-VP	0.370	0.514

## Results

**Titration Characteristics of Polymer Catalysts.** As in the accompanying paper,<sup>5</sup> p*K*<sub>a</sub> and p*K*<sub>int</sub> values of the imidazole group were determined from eq 1 and

$$pK_a = pH + n' \log [(1 - \alpha)/\alpha] \quad (1)$$

eq 2, respectively, where  $\Delta G_{el}$  is the required electro-

$$pK_{app} = pH + \log [(1 - \alpha)/\alpha] =$$

$$pK_{int} + 0.43\Delta G_{el}/RT \quad (2)$$

static energy for the removal of an equivalent of protons at a given degree of ionization. The p*K* values obtained are summarized in Table III, together with

**Table III.** Titration Characteristics of Polymer Catalysts<sup>a</sup>

Copolymer	Temp, °C	p <i>K</i> <sub>a</sub>	<i>n</i> '	p <i>K</i> <sub>int</sub>
PI-AA-1	20	6.15	1.09	
PI-AA-1	30	6.09	1.09	6.18
PI-AA-1	40	6.01	1.01	
PI-AA-2	20	5.97	1.22	
PI-AA-2	30	5.85	1.24	6.08
PI-AA-2	40	5.77	1.31	
PI-AP-AA-1	30	6.16	1.14	6.28
PI-AP-AA-2	30	6.17	1.14	6.25
PI-VP	15	5.88	0.99	
PI-VP	20	5.83	1.00	
PI-VP	30	5.70	0.98	5.74
PI-VP	40	5.60	1.01	

<sup>a</sup> 1.0 *M* aqueous KCl.

*n*' values, the deviation of which from unity can be used as a qualitative measure of the electrostatic effect.

The titration behavior of these copolymers is in general similar to that observed in benzimidazole (BI)-containing copolymers. Thus the PI-AA copolymer possessed *n*' values of greater than one, showing electrostatic repulsion operating among the charged phenyl-imidazole units. The *n*' value increased with an increase in the content of the PI unit. The *n*' value for the PI-AA-2 copolymer (PI unit, 8.9 mol %) was 1.24 at 30°C. This value is smaller than that (*n*' = 1.56) observed for a BI-AA copolymer (BI unit, 7.8 mol %).<sup>5</sup> The difference is explained by a greater extent of intramolecular association of the BI unit, hence a greater electrostatic

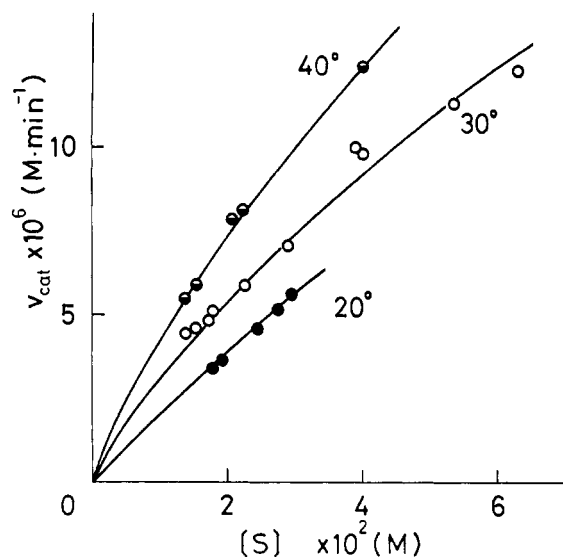


Figure 1. Catalytic hydrolysis: catalyst, PI-AA-1; imidazole concentration, 1.55 mM; pH 8.0; 1.0 M aqueous KCl.

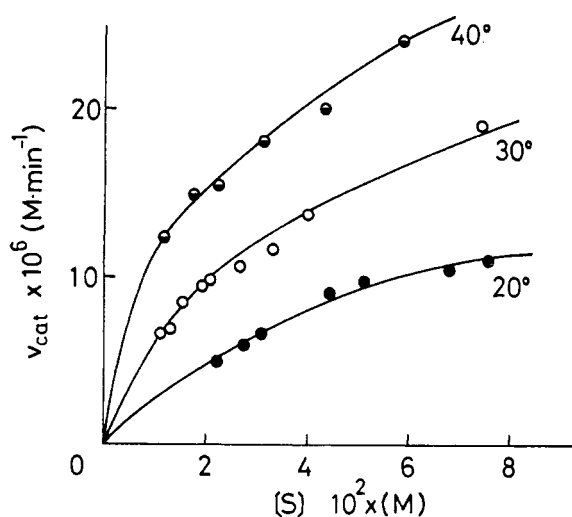


Figure 2. Catalytic hydrolysis: catalyst, PI-AA-2; imidazole concentration, 0.83 mM; pH 8.0; 1.0 M aqueous KCl.

interaction. The terpolymers containing the AP unit (PI-AP-AA) showed smaller electrostatic interaction, and there was no indication of the electrostatic effect in the PI-VP copolymer ( $n' \approx 1$ ).

**Catalytic Hydrolyses with Polymer Catalysts.** In Figures 1–3 are shown the variation of the rate of catalytic hydrolysis  $v_{\text{cat}}$  with substrate concentration for the PI-AA and PI-VP copolymers at several temperatures. The saturation phenomena of  $v_{\text{cat}}$  were not very clear in Figure 1; in particular it was difficult to detect at 20°. Thus the PI unit, if isolated, appears to show only a small binding capability toward substrate. As the content of the PI unit increased from 1.7 to 8.9 mol % in the copolymer, saturation phenomena were observed more clearly as shown in Figure 2. The PI-VP copolymer showed similarly sufficient substrate saturation. Unlike the BI-VP copolymer, the PI-VP copolymer did not show a rate acceleration phenomenon which is ascribable to accumulation of phenol molecules in the reaction mixture.

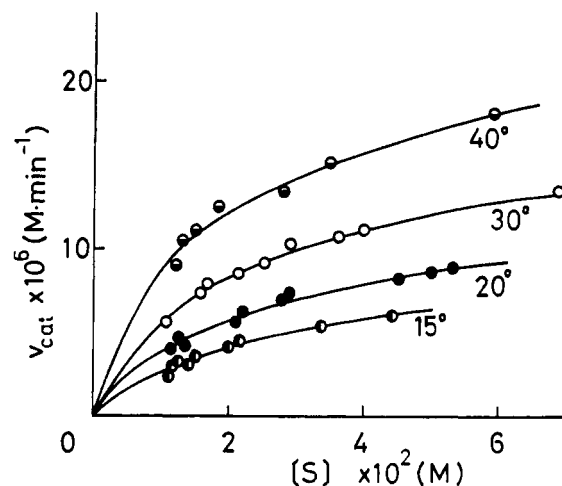
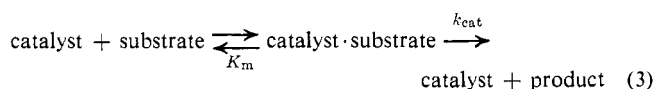


Figure 3. Catalytic hydrolysis: catalyst, PI-VP; imidazole concentration, 1.32 mM; pH 8.0; 1.0 M aqueous KCl.

The data are described satisfactorily by Michaelis-Menten kinetics (eq 3), as in the polymer catalysis in-



$$v_{\text{cat}} = \frac{k_{\text{cat}}[C][S]}{K_m + [S]} \quad (4)$$

vestigated previously.<sup>1b,5</sup> The kinetic parameters,  $K_m$  and  $k_{\text{cat}}$ , can be determined from the linear Lineweaver-Burk plot between  $1/v_{\text{cat}}$  and  $1/[S]$ .<sup>7</sup> The Michaelis constant  $K_m$  can be assumed to represent a true dissociation constant of catalyst and substrate<sup>1b</sup> and the  $k_{\text{cat}}$  term is related to the substrate turnover, because the mole of the acid released in the initial portion of the added alkali *vs.* time curve was greater than that of the catalyst used. The kinetic parameters obtained are summarized in Table IV. In the absence of clear-

Table IV. Catalytic Hydrolyses with Polymer Catalysts<sup>a</sup>

Polymer	Temp, °C	$K_m$ , mM	$k_{\text{cat}}$ , min <sup>-1</sup> × 10 <sup>3</sup>	$k_{\text{cat}}/K_m$ , min <sup>-1</sup> M <sup>-1</sup>
PI-AA-1	20			( $k' = 0.12$ )
PI-AA-1	30	83	19	0.23
PI-AA-1	40	48	24	0.50
PI-AA-2	20	38	20	0.51
PI-AA-2	30	29	29	1.02
PI-AA-2	40	22	38	1.72
PI-AP-AA-1 <sup>b</sup>	30	14	14	0.95
PI-AP-AA-1 <sup>c</sup>	30	10	12	1.19
PI-AP-AA-2 <sup>d</sup>	30	12	17	1.39
PI-VP	15	24	7.8	0.32
PI-VP	20	22	9.3	0.43
PI-VP	30	19	13	0.66
PI-VP <sup>e</sup>	30	19	12	0.59
PI-VP	40	17	18	1.04

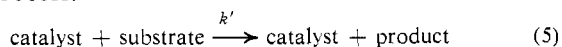
<sup>a</sup> At pH 8.0 in 1 M aqueous KCl unless otherwise noted. See Figures 1–3 for the total imidazole concentration if not given.

<sup>b</sup> Total imidazole concentration, 0.84 mM. <sup>c</sup> At pH 7.0 in 1 M aqueous KCl; total imidazole concentration, 0.84 mM; the fraction of the neutral imidazole unit, 87.4%. <sup>d</sup> Total imidazole concentration, 0.82 mM. <sup>e</sup> At pH 7.0 in 1 M aqueous KCl; total imidazole concentration, 1.32 mM; the fraction of the neutral imidazole unit, 95.2%.

(7) H. Lineweaver and D. Burk, *J. Amer. Chem. Soc.*, **56**, 658 (1934).

cut substrate saturation, the catalytic process with the PI-AA-1 catalyst may consist of both the bimolecular and enzyme-like pathways, and the interpretation of the kinetic parameters obtained would become ambiguous. Thus these data were not used for discussions of the thermodynamic and activation parameters. The data with the PI-AA-1 copolymer at 20° was expressed by the second-order kinetics (eq 5 and 6), and a second-order rate constant  $k' = 0.12 \text{ min}^{-1} \text{ M}^{-1}$  is given instead of  $K_m$  and  $k_{\text{cat}}$ . The smaller binding capacity of the PI unit relative to the BI unit is shown by comparing  $K_m$  values. The  $K_m$  value of a BI-AA copolymer (BI unit, 1.3 mol %) was 53 mM at 30° and that of a PI-AA copolymer of comparable composition was 83 mM. In Table IV are also included kinetic parameters for the catalytic hydrolysis with the PI-AP-AA terpolymer at 30°. The incorporation of the AP unit increased the binding capacity of the AA polymer. The data of the catalytic hydrolysis at pH 7.0 are also included. The kinetic parameters for PI-VP polymer were the same at pH 8.0 and 7.0 (protonation of the imidazole group was corrected). In contrast, a PI-AP-AA catalyst showed two times greater binding capacity at pH 7.0 than at pH 8.0.

**Catalytic Hydrolyses with Imidazole Derivatives.** The rate of the catalytic hydrolysis with AcPI catalyst increased proportionally with substrate concentration (0.01–0.07 M) in the temperature range of 15–40°. Thus the reaction pathway with this catalyst is a second-order process.



$$v_{\text{cat.}} = k'[\text{C}][\text{S}] \quad (6)$$

The same catalytic pathway was observed with imidazole as catalyst at 15–40°. These data are summarized in Table V.

Table V. Catalytic Hydrolyses<sup>a</sup>

Catalyst	Temp, °C	pK <sub>a</sub>	Catalyst concn, mM	$k'$ , min <sup>-1</sup> M <sup>-1</sup>
AcPI	15	6.21	1.95	0.096
AcPI	20	6.16	1.95	0.12
AcPI	30	6.18	1.95	0.27
AcPI	40	6.06	1.95	0.43
Imidazole	20	7.21	4.80	0.24
Imidazole <sup>b</sup>	30	7.13	27.9	0.33
Imidazole	40	7.06	5.35	0.61

<sup>a</sup> pH 8.0; 1.0 M aqueous KCl. <sup>b</sup> From ref 3.

Previously we showed that imidazole derivatives containing naphthalene groups (1, 2) catalyzed the hydro-

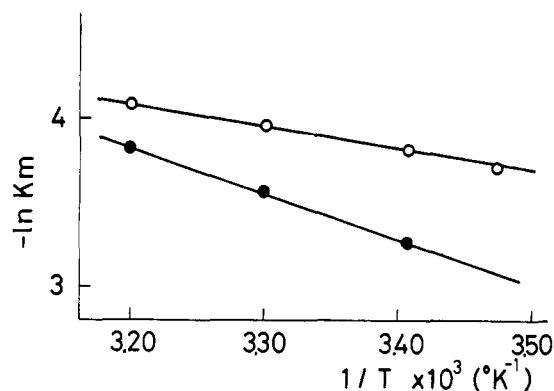
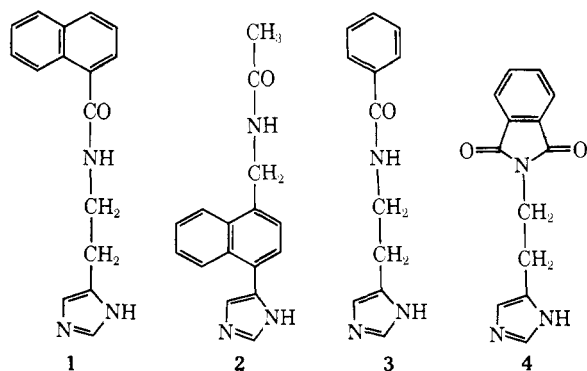


Figure 4. Temperature dependence of substrate binding: ●, PI-AA-2; ○, PI-VP.

lysis of the same substrate, *p*-acetoxybenzoic acid, according to Michaelis–Menten kinetics, whereas imidazole catalysts with the benzene ring (3, 4) catalyzed the hydrolysis following second-order kinetics.<sup>4</sup> The present data are consistent with these results, showing that the benzene derivatives are not sufficiently hydrophobic to bind the substrate prior to catalysis under the hydrolysis condition employed.

**Thermodynamic and Activation Parameters of Catalytic Hydrolysis.** The thermodynamic parameters for the binding process were obtained for catalyses with PI-AA-2 and PI-VP copolymers. Figure 4 shows the plots between  $\ln K_m$  and  $1/T$ . Linear relationships are obtained and the enthalpic and entropic changes of the binding of catalyst and substrate are calculated from the equation

$$\Delta G = -RT \ln (1/K_m) \quad (7)$$

$$= \Delta H - T\Delta S \quad (8)$$

The binding process was associated with positive enthalpy changes and large positive entropy changes. These data are given in Table VI, together with the data

Table VI. Thermodynamic Parameters for Substrate Binding

Catalyst	$\Delta H$ , kcal/mol	$\Delta S$ , eu	$\Delta S_u$ , eu	$\Delta G_u(303^\circ\text{K})$ , kcal/mol
PI-AA-2	5.40	24.9	32.9	-4.57
PI-VP	1.20	11.8	19.8	-4.80
1 <sup>a</sup>	3.74	20.5	28.5	-4.90
2 <sup>a</sup>	3.44	19.9	27.9	-5.01

<sup>a</sup> From ref 4.

for naphthylimidazole catalysts. The unitary free energy and entropy changes were obtained from the following relations.<sup>8</sup>

$$\Delta G_u = \Delta G - 7.98T \quad (9)$$

$$\Delta S_u = \Delta S + 7.98 \quad (10)$$

The free energy of activation was calculated for the intracomplex and second-order rate processes from eq 11<sup>9</sup> and plotted against  $T$ . Satisfactory linear relation-

$$\Delta G^\ddagger = RT \ln (kT/hk_r) \quad (11)$$

$$= \Delta H^\ddagger - T\Delta S^\ddagger \quad (12)$$

(8) W. Kauzmann, *Advan. Protein Chem.*, **14**, 1 (1959).

(9) A. A. Frost and R. G. Pearson, "Kinetics and Mechanisms," 2nd ed, Wiley, New York, N. Y., 1961, p 98.

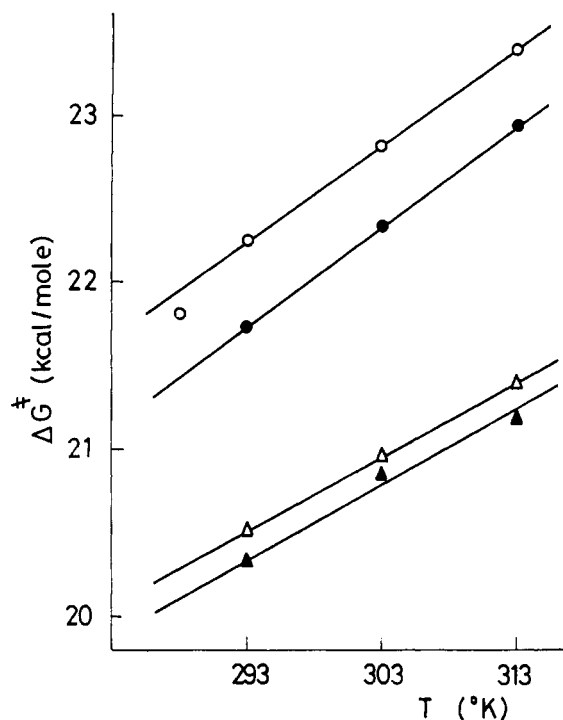


Figure 5. Temperature dependence of the free energy of activation:  $\Delta G^\ddagger$  was calculated from the respective rate constant; O, PI-VP catalyst, intracomplex process ( $k_{\text{cat}}$ ); ●, PI-AA-2 catalyst, intracomplex process ( $k_{\text{cat}}$ ); Δ, AcPI catalyst, second-order process ( $k'$ ); ▲, imidazole catalyst, second-order process ( $k'$ ).

ships resulted as shown in Figure 5. The plot at 15° deviated from linearity. The enthalpy and entropy of activation were obtained from intercept and slope, respectively (eq 12), and are given in Table VII. The

Table VII. Activation Parameters of the Intracomplex and Bimolecular Processes

Catalyst	Catalytic process <sup>a</sup>	$\Delta H^\ddagger$ , kcal/mol	$\Delta S^\ddagger$ , eu	$\Delta G^\ddagger(303^\circ\text{K})$ , kcal/mol
PI-AA-2	I	4.17	-60.0	22.35
PI-VP	I	5.26	-58.0	22.83
1 <sup>b</sup>	I	7.31	-50.4	22.55
2 <sup>b</sup>	I	6.26	-52.0	21.96
AcPI	B	7.66	-44.0	20.99
Imidazole	B	6.19	-48.5	20.89
3 <sup>b</sup>	B	6.43	-47.0	20.64

<sup>a</sup> I, intracomplex process; B, bimolecular process. <sup>b</sup> From ref 4.

corresponding data in the previous publication<sup>4</sup> are also listed for comparison. It is interesting that the intracomplex process in the polymer catalyst shows smaller  $\Delta H^\ddagger$  values (by 1–3 kcal/mol) and greater  $\Delta S^\ddagger$  values (by 6–10 eu) than those of the small molecule catalysts.

## Discussion

**Catalytic Hydrolysis.** The catalytic behavior of the polymer catalyst containing the PI unit was generally similar to that of the benzimidazole-containing copolymer. Thus Michaelis-Menten kinetics were observed for the polymer catalysts except for the catalysis by the PI-AA-1 copolymer at 20°.

It is interesting that the copolymer composition affected the catalytic behavior of the BI-AA and PI-AA copolymers differently. In the BI-AA copolymer,

the increase in the amount of the BI unit from 1.3 to 7.8 mol % resulted in a small decrease in the binding capacity ( $K_m$ ; 53 vs. 77 mM) and  $k_{\text{cat}}$  did not vary. These results were explained by the supposition that the flat benzimidazole ring, when associated, may assume a plane-to-plane conformation which is not favorable for creation of the cooperative catalytic site.<sup>5</sup> In contrast, formation of a catalytic site of different structure may be expected by aggregation of less rigid phenylimidazole groups. The increase in the PI content from 1.7 to 8.9 mol % caused increases both in binding capacity ( $K_m$ ; 83 vs. 29 mM) and in the intracomplex rate constant ( $k_{\text{cat}}$ ;  $19 \times 10^{-3}$  vs.  $29 \times 10^{-3} \text{ min}^{-1}$ ). Thus, it is possible that a cooperative multifunctional catalytic site was formed by flexible association of the PI unit. Particularly interesting in this regard is the fact that the enthalpy of activation for PI-AA-2 catalyst, 4.2 kcal/mol, is smaller than those of the related catalysts (see Table VII).

The decrease in the enthalpy of activation in the polymer catalysis has been observed in a related system. Overberger, *et al.*,<sup>10</sup> found that enthalpies of activation of the catalytic hydrolysis (the second-order process) of *p*-nitrophenyl acetate with polyvinylimidazole and polyvinylbenzimidazole were smaller than those with the corresponding small imidazole molecules. The bifunctional catalysis by the polymer catalyst was considered to be responsible for the difference.

In the accompanying paper we mentioned that the BI-VP copolymer forms a fairly loose catalytic loop and that substrate and phenol molecules can be included in an expanded catalytic loop to give rise to a cooperative catalytic site. The tightness of a catalytic loop conceivably increases as the relative contribution of the neighboring VP unit to substrate binding increases. The  $K_m$  ratio of the VP copolymer to the AA copolymer is greater for the PI polymer (~4) than for the BI polymer (~3), hence a greater contribution of the VP unit to substrate binding in the PI polymer than in the BI polymer. The catalytic loop of the PI-VP copolymer is apparently tighter than that of the BI-VP copolymer, and, consequently, cannot accommodate substrate and additive molecule simultaneously. Thus rate acceleration due to bound phenols will not be observed.

**Isoequilibrium and Isokinetic Relationships.** The association of nonpolar groups due to hydrophobic forces in aqueous environment is known to be accompanied by a large positive entropy change and a small enthalpy change.<sup>8</sup> The thermodynamic parameters obtained with the polymer catalyst clearly indicate that hydrophobic forces are responsible for substrate binding. The smaller  $\Delta S_a$  value (19.8 eu) for the PI-VP copolymer relative to that (32.9 eu) of the PI-AA-2 copolymer probably reflects different modes of substrate binding of these polymers. In the previous paper we suggested that VP copolymers formed catalytic loops upon substrate binding and that the catalytic site of the AA copolymer was relatively fixed.<sup>5</sup> Since the loop formation is entropically unfavorable, the entropy increase due to the hydrophobic interaction with substrate becomes partially compensated in the VP copolymer, as shown by the  $\Delta S_a$  value.

(10) C. G. Overberger, T. St. Pierre, C. Yaroslavsky, and S. Yaroslavsky, *J. Amer. Chem. Soc.*, **88**, 1184 (1966).

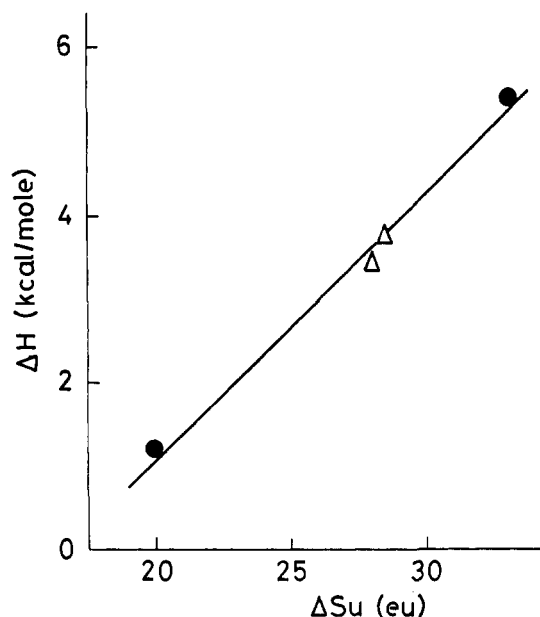


Figure 6. Isoequilibrium relationship in substrate binding: ●, polymer catalysts; △, small molecule catalysts.

The enthalpy changes for substrate binding are plotted against the corresponding unitary entropy changes in Figure 6. The thermodynamic data of a previous publication<sup>4</sup> are also employed. A satisfactory linear relation was obtained. Thus an isoequilibrium relationship<sup>11</sup>

$$\delta\Delta H = \beta\delta\Delta S_u \quad (13)$$

holds for substrate binding, and it is indicated that a single interaction mechanism is predominant for this process. The isoequilibrium temperature  $\beta$  determined from the slope was  $320 \pm 20^\circ\text{K}$ . The  $\beta$  value obtained is consistent with the supposition that the binding process is primarily based on hydrophobic forces. Molyneux and Frank<sup>12</sup> observed a linear relationship between  $\Delta H$  and  $\Delta S_u$  of binding of aqueous polyvinylpyrrolidone with organic substances, and the slope of the line,  $340^\circ\text{K}$ , was considered to indicate the "melting point of icebergs." These two sets of data can be plotted on almost the same line. Since it has been already shown that anomalous behavior of water based on its structuredness vanishes at around  $70^\circ$ ,<sup>13</sup> the substrate binding must be closely related to the structure of water, further supporting the occurrence of the hydrophobic interaction between catalyst and substrate.

In Figure 7 are plotted the enthalpy of activation of the catalytic process against the corresponding entropy of activation. The isokinetic relationship<sup>11</sup>

$$\delta\Delta H^\ddagger = \beta'\delta\Delta S^\ddagger \quad (14)$$

appears to hold for the three plots for the second-order process. The isokinetic temperature was  $350^\circ\text{K}$ , and a single interaction mechanism is conceivably operating for this process. On the other hand, the plots for the

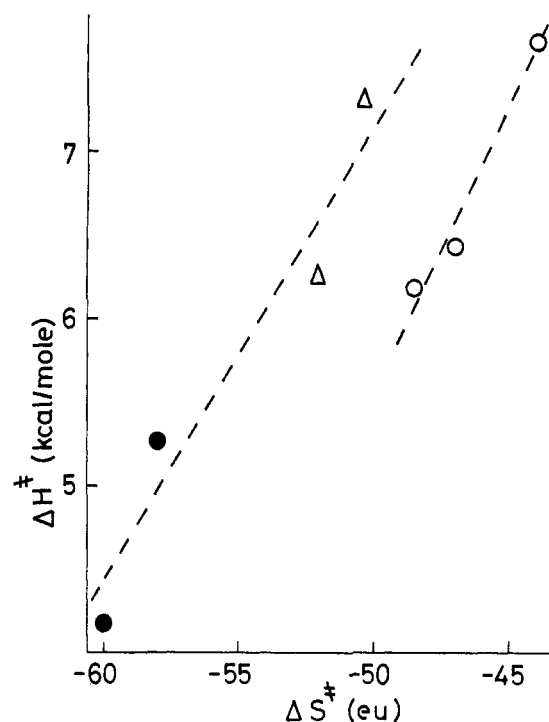


Figure 7. Isokinetic relationships in catalytic processes: ●, intra-complex process (polymer catalysts); △, intracomplex process (small molecule catalysts); ○, bimolecular process.

intracomplex process were somewhat scattered. It is possible that the plots for the polymer catalyst lie on a line different from that for the small molecule catalysts (1 and 2). The mechanism of the enzyme-like catalytic process may be different between these two types of catalysts. This is more clearly shown in the  $\Delta G^\ddagger_{\text{corr}} - \Delta G_u$  plot given below.

**Intracomplex Process.** As mentioned in the accompanying paper,<sup>5</sup> the intracomplex process involves either general-base or nucleophilic catalysis. The  $k_{\text{cat}}$  term represents the true turnover constant in the case of general-base catalysis, whereas it is composed of the rates of acylation and deacylation in the case of nucleophilic catalysis.<sup>14</sup>

$$k_{\text{cat}} = \frac{k_{\text{acyl}}k_{\text{deacyl}}}{k_{\text{acyl}} + k_{\text{deacyl}}} \quad (15)$$

The rate of the catalytic hydrolysis with AcPI catalyst was first order with respect to substrate. AcPI, like imidazole, most probably acts as a nucleophilic catalyst in the overall second-order process,<sup>15</sup> and the kinetic data obtained indicate that there was no accumulation of the acetylimidazole intermediate in the reaction mixture, *i.e.*, deacylation is not rate limiting. The situation is probably the same in the intracomplex process. The catalytic hydrolysis of 3-acetoxy-*N*-trimethylanilinium iodide (ANTI) with PI-VP catalyst proceeded according to Michaelis-Menten kinetics and  $k_{\text{cat}}$  ( $30^\circ$ , pH 8.0, 1.0 M KCl) was  $0.025 \text{ min}^{-1}$ .<sup>16</sup> This rate is two times greater than  $0.013 \text{ min}^{-1}$  observed for *p*-acetoxybenzoic acid under the identical condition. These results require that deacylation is not rate lim-

(11) J. E. Leffler and E. Grunwald, "Rates and Equilibria of Organic Reactions," Wiley, New York, N. Y., 1963, Chapter 9.

(12) P. Molyneux and H. P. Frank, *J. Amer. Chem. Soc.*, **83**, 3169 (1961).

(13) *E.g.*, G. Némethy and H. A. Scheraga, *J. Chem. Phys.*, **36**, 3382 (1962).

(14) B. Zerner and M. L. Bender, *J. Amer. Chem. Soc.*, **86**, 3669 (1964).

(15) T. C. Bruice and S. J. Benkovic, "Bioorganic Mechanisms," Vol. 1, W. A. Benjamin, New York, N. Y., 1966, Chapter 1.

(16) T. Kunitake and S. Shinkai, in preparation.

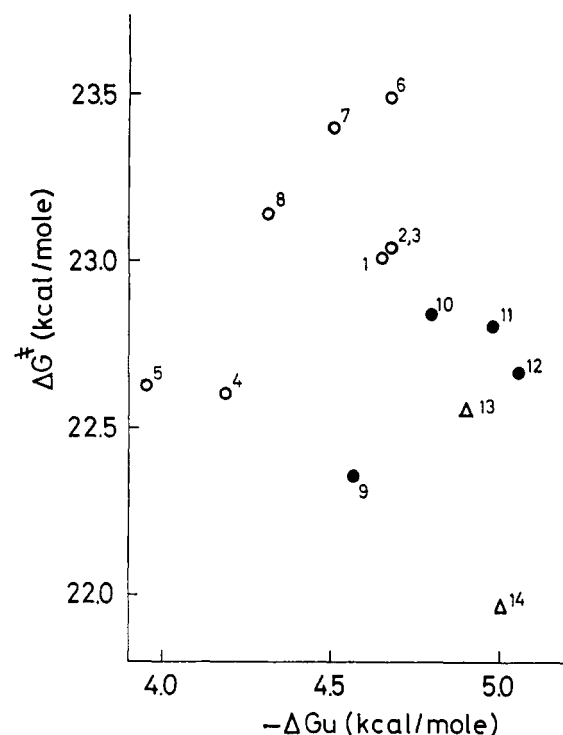


Figure 8. Correlation of free energies of binding and activation. The data obtained at 30° and pH 8.0 (ref 5 and this paper) are employed. For catalysts 1–8, see ref 5: 1, BI-VP-1; 2, BI-VP-2; 3, BI-VP-3; 4, BI-AA-1; 5, BI-AA-2; 6, BI-AP-AA-1; 7, BI-AP-AA-2; 8, BI-AP-AA-3; 9, PI-AA-2; 10, PI-VP; 11, PI-AP-AA-1; 12, PI-AP-AA-2; 13, 1; 14, 2.

iting, because  $k_{\text{cat}}$  would be identical if decomposition of the acetylimidazole intermediate was rate limiting.

From these discussions it is evident that  $k_{\text{cat}} \approx k_{\text{acyl}}$ , since  $k_{\text{acyl}} < k_{\text{deacyl}}$  (eq 15) in the case of nucleophilic catalysis, though the possible influence of the rate of deacylation on  $k_{\text{cat}}$  cannot be totally discarded at present.

In the first paper of this series it was mentioned that "formation of the charged acylimidazole intermediate in the case of nucleophilic catalysis might not be favored in the predominantly hydrophobic site of catalysis."<sup>1b</sup> Speaking more generally, the increased polarity of the transition state relative to that of ground state should decrease the rate of the intracomplex reaction occurring in hydrophobic environments. Compensation of the binding tendency and intracomplex rates is qualitatively noted in the data of Table IV.

The existence or nonexistence of the correlation between the binding capacity and the catalytic efficiency of an active site is an interesting problem in the enzymatic catalysis. For example, it was noted that there was no parallel between substrate binding and catalytic rate for an extensive series of substrates in the  $\alpha$ -chymotrypsin catalysis.<sup>17</sup> A more limited correlation, however, was observed in the  $\alpha$ -chymotrypsin-catalyzed hydrolysis of acylated amino acid esters.<sup>18</sup> Thus we attempted to find such a correlation and plotted the free energy of activation  $\Delta G^\ddagger$  vs. the unitary free energy of substrate binding  $\Delta G_u$  for the enzyme-like hydrolysis of *p*-acetoxybenzoic acid with various imidazole-containing cat-

(17) G. Hein and C. Niemann, *Proc. Nat. Acad. Sci. U. S.*, **47**, 1341 (1961).

(18) J. Bryan Jones, T. Kunitake, C. Niemann, and G. Hein, *J. Amer. Chem. Soc.*, **87**, 1777 (1965).

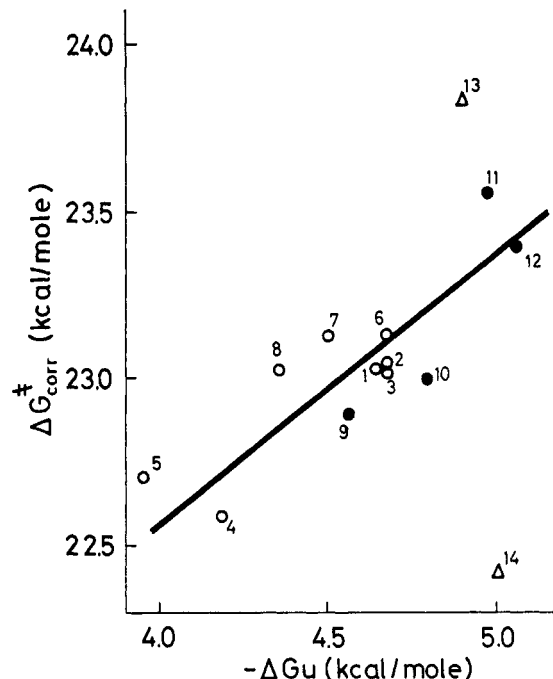


Figure 9. Correlation of free energies of binding and activation. The data are the same as in Figure 8. The contribution of the nucleophilic reactivity to the free energy of activation was corrected.

alysts. Figure 8 gives the plots. It is apparent that there is no correlation in the plots.

The intracomplex rate of the imidazole catalysis is considered to be determined primarily by the nucleophilicity of the imidazole group and by the nature of the binding site. Bruice and Schmir<sup>19</sup> found that the rate of nucleophilic attack  $k_N$  of imidazoles was related to their acid dissociation constants  $pK_a$  by the equation

$$\log k_N = 0.8pK_a - 4.30 \quad (16)$$

in the imidazole-catalyzed hydrolysis of *p*-nitrophenyl acetate. If we assume an analogous relationship holds for the intracomplex catalysis, the  $\Delta G^\ddagger$  value which would be observed if the imidazole group possessed  $pK_a = 5.60$  (an arbitrary reference point) is given by the equation

$$\Delta G_{\text{corr}}^\ddagger = \Delta G^\ddagger + 0.8(pK_a - 5.60) \times 2.303RT \quad (17)$$

In the case of polymer catalysts,  $pK_{\text{int}}$  (eq 2) must be employed instead of  $pK_{\text{app}}$ . Since the influence of the intrinsic nucleophilicity of imidazoles is corrected, the  $\Delta G_{\text{corr}}^\ddagger$  term may represent the variation of the activation energy of the intracomplex process with the nature of the binding site. Figure 9 shows the relation of  $\Delta G_{\text{corr}}^\ddagger$  and  $\Delta G_u$ . Apparently  $\Delta G_{\text{corr}}^\ddagger$  and  $\Delta G_u$  for polymer catalysts are correlated fairly well, whereas plots for small-molecule catalysts deviated considerably. This deviation suggests that the course of the enzyme-like pathway is different from that of the polymer catalyst. The line obtained for the polymer catalyst by the least squares method is given by

$$\Delta G_{\text{corr}}^\ddagger = -0.82\Delta G_u + 18.9 \quad (18)$$

This correlation suggests several interesting features of the present catalytic systems. As mentioned above, the binding process was governed primarily by hydro-

(19) T. C. Bruice and G. L. Schmir, *ibid.*, **80**, 148 (1958).

phobic forces, and, therefore,  $\Delta G_u$  can be a measure of the extent of the hydrophobic interaction between catalyst and substrate. Since  $\Delta G_{\text{corr}}^\ddagger$  and  $\Delta G_u$  are inversely correlated, it can be said that the transition state (probably charged) of the intracomplex process is destabilized increasingly as the extent of the hydrophobic interaction increases. It seems that the structural variation (modes of intramolecular aggregation) *per se* of the polymer catalytic site as discussed in the previous paper<sup>5</sup> plays a secondary role in influencing the catalytic efficiency. Scatters in Figure 9 may represent the more subtle influence of the nature of the catalytic site apart from hydrophobicity, in addition to insufficient correction of the nucleophilicity of imidazole.

As mentioned above, a small  $\Delta H^\ddagger$  value of PI-AA-2 polymer relative to other catalysts may indicate the co-operative catalytic action of this polymer. However, the plot for this polymer in Figure 9 does not deviate much from the linear relationship. Since an enthalpy decrease due to the cooperative catalysis of functional groups is often accompanied by an entropy increase, the free energy of activation may not be necessarily decreased by the occurrence of the bifunctional catalysis. On the other hand, it is also possible that the activation parameters observed are related to the geometrical structure of the catalytic site rather than to the occurrence of the bifunctional catalysis. Additional data are needed in order to assert the presence of the cooperative action in the PI-AA polymer.

Equation 18 further indicates that the decrease in  $\Delta G_u$  is comparable to the increase in  $\Delta G_{\text{corr}}^\ddagger$ . This means that stabilization of the catalyst-substrate complex gives rise to the corresponding destabilization of the transition state of the intracomplex process. This situation is shown by the reaction profile of Figure 10. In this diagram the gain in free energy by increased binding ( $\Delta G_{u2} - \Delta G_{u1}$ ) is compensated considerably ( $\sim 82\%$ ) by the increase in activation energy ( $\Delta G_2^\ddagger - \Delta G_1^\ddagger$ ). Explicit in this diagram is the fact that the energy levels of the transition states are close, irrespective of the stability of the catalyst-substrate complex. We consider that the hydrophobic interaction between catalyst and substrate has to be mostly destroyed for the intracomplex reaction to occur, thus compensating the difference in the stability of the catalyst-substrate complex and leading to similar transition states. As shown in Table VII, the activation entropies of the intracomplex process were extraordinarily large negative values ( $-58$  to  $-60$  eu). These results are contrary to the expectation that the intracomplex reaction will be favored entropically. For example, it has been found that the intramolecular catalysis is favored entropically by 15–20 eu in several displacement reactions on phenyl esters.<sup>15</sup> Although the unfavorable geometrical arrangement of catalyst and substrate in the Michaelis complex for the catalytic action may contribute to the decrease in  $\Delta S^\ddagger$ ,<sup>4</sup> the above discussion indicates strongly that the large negative  $\Delta S^\ddagger$  value was caused primarily by the breaking of the hydrophobic interaction in the transition state.

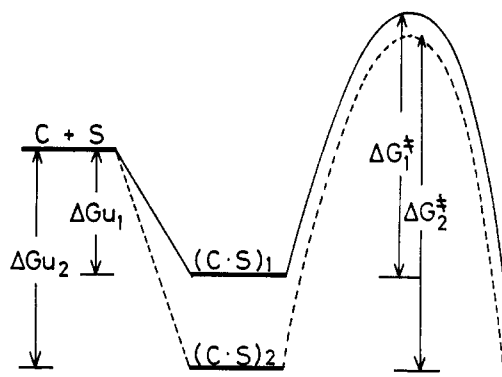


Figure 10. Free energy diagram of the enzyme-like catalysis.

The  $\Delta G_{\text{corr}}^\ddagger$  value at  $\Delta G_u = 0$  was 18.9 kcal/mol in eq 18. This value is smaller than the free energy of activation for the second-order process ( $\Delta G^\ddagger$  corrected to pH 5.60; 21–22 kcal/mol). The difference clearly shows the better catalytic efficiency of the enzyme-like pathway relative to the second-order pathway.

## Conclusion

In the accompanying paper,<sup>5</sup> we illustrated representative structures of the polymer catalytic site, as formed by intramolecular aggregation. We expected previously that the rate of the intracomplex process would be highly influenced by the structural variation of the catalytic site. The correlation of  $\Delta G_{\text{corr}}^\ddagger$  and  $\Delta G_u$  shown in Figure 9, however, indicates that the catalytic property was largely determined by the hydrophobicity of the catalytic site, apart from the nucleophilicity of imidazole groups. Thus the structural difference of the catalytic site was not directly related to the catalytic efficiency. In these systems the substrate molecule is rather small and is conceived to be surrounded fairly completely by the polymer catalyst. The structure-reactivity relationship may be quite different if the binding portion of the substrate is somewhat more removed from the reacting portion than in *p*-acetoxybenzoic acid.

In the present investigation, the hydrophobic interaction was the predominant interaction mechanism between catalyst and substrate. A greater selectivity was observed when electrostatic forces in combination with hydrophobic forces were utilized for substrate binding.<sup>16</sup> Thus we believe that combinations of various secondary valence forces would be particularly effective for selective substrate binding. Investigations are being carried out on syntheses of catalytic systems of higher selectivity and efficiency.

**Acknowledgment.** We are very grateful to Professor Chuji Aso, head of our research group, for his unfailing encouragement and advice. We also appreciate very much the capable assistance of Miss Fumiko Shimada and Mr. Yoshiyuki Tanaka in the preparation of imidazole compounds.